

Research Article

How to cite this article:

Atazadeh S, Hasan Sadeh M, Farokhi F, Ahmadian S, Saghati S, Valipour F, Fattahi A, Tamadon A, Rahbarghazi R, Mahdipour M. Autophagy Modulation Influenced the Spermatogenesis in Rodent Testicular Organoids and Diabetic Condition. *Advanced Pharmaceutical Bulletin*, doi: 10.34172/apb.46240

**Autophagy Modulation Influenced the Spermatogenesis in Rodent Testicular Organoids and Diabetic Condition**

Shadi Atazadeh<sup>1§</sup>, Maryam Hasan Sadeh<sup>1§</sup>, Farah Farokhi<sup>2\*</sup>, Shahin Ahmadian<sup>1</sup>, Sepideh Saghati<sup>1</sup>, Fereshteh Valipour<sup>3</sup>, Amir Fattahi<sup>4</sup>, Amin Tamadon<sup>5</sup>, Reza Rahbarghazi<sup>1,6</sup>, Mahdi Mahdipour<sup>1,4\*</sup>

<sup>1</sup>Stem Cell Research Center, Tabriz University of Medical Sciences, Tabriz, Iran

<sup>2</sup>Department of Biology, Faculty of Science, Urmia University, Urmia, Iran

<sup>3</sup>Department of Medicinal Chemistry, Faculty of Pharmacy, Tabriz University of Medical Sciences, Tabriz, Iran

<sup>4</sup>Department of Reproductive Biology, Faculty of Advanced Medical Sciences, Tabriz University of Medical Sciences, Tabriz, Iran

<sup>5</sup>Department of Natural Sciences, West Kazakhstan Marat Ospanov Medical University, Aktobe, Kazakhstan

<sup>6</sup>Department of Applied Cell Sciences, Faculty of Advanced Medical Sciences, Tabriz University of Medical Sciences, Tabriz, Iran

ARTICLE INFO

ABSTRACT

**Keywords:**

Alginate/gelatin hydrogel,  
Testicular organoids,  
Autophagy,  
Diabetes Mellitus,  
Spermatogenesis

**Article History:**

Submitted: August 17, 2025

Revised: May 20, 2026

Accepted: June 22, 2026

ePublished: June 29, 2026

**Purpose:** Here, the effect of autophagy activity was investigated in rat testicular organoids embedded in alginate/gelatin (Alg/Gel) hydrogel. Additionally, we monitored the spermatogenesis potential in diabetic mice following the administration of metformin (Met) and/or hydroxychloroquine (HCQ). **Methods:** Alg/Gel hydrogel was fabricated, and its physicochemical properties were studied. The survival rate of freshly isolated rat whole testicular tissue cells being plated on the Alg/Gel hydrogel surface was monitored after 7 days. Rat testicular organoids were embedded in Alg/Gel hydrogel and exposed to 15  $\mu$ M HCQ and/or 5  $\mu$ M Met for 7 days. Histological examination was conducted to assess OCT3/4+ progenitors and maturing sperm cells. Using western blotting, the levels of autophagic markers Beclin-1, LC3, and P62 were evaluated. Diabetic mice received 120 mg/kg body weight Met and/or 70 mg/kg bodyweight HCQ for 4 weeks, followed by histological examinations and sperm analysis. **Results:** The fabricated Alg/Gel hydrogel demonstrated suitable physicochemical properties, which correlated with an increased survival rate of whole testicular tissue cells compared to the control group ( $p < 0.05$ ). Data indicated a promotion of autophagy (Beclin-1 $\uparrow$ , LC3-II-I ratio $\uparrow$ , P62 $\downarrow$ ) and an inhibition of autophagy (LC3 $\downarrow$ ) in testicular organoids after treatment with Met and HCQ, respectively, compared to the control group ( $p < 0.05$ ). These changes were accompanied by an induction of SOD activity in Met-treated testicular organoids ( $p < 0.05$ ). In the presence of Met and HCQ, OCT3/4+ progenitors were reduced in rat organoids compared to non-treated control organoids ( $p < 0.05$ ). Administration of Met, but not HCQ, in diabetic mice was able to restore some sperm parameters, such as motility, and reduce abnormal morphologies compared to the matched diabetic mice ( $p < 0.05$ ).

**Conclusions:** Regulation of autophagy can influence spermatogenesis capacity, affecting seminiferous tubule progenitors, maturation, and sperm parameters. In studies of rat testicular organoids and diabetic mice, these findings suggest that the autophagy response is a promising signaling pathway target in subfertile or infertile males.

§ These authors contributed equally to this work and are considered the co-first authors

**\*Corresponding Author**

Mahdi Mahdipour, Email: mahdi.mahdipour@gmail.com, ORCID: 0000-0002-2729-4593

Farah Farokhi, Email: f.farokhi@urmia.ac.ir

## Introduction

Infertility is a global clinical issue with the inability to conceive after 12 months of unprotected intercourse.<sup>1</sup> Infertility can affect both males and females of reproductive age with socioeconomic burdens.<sup>2</sup> In males, genetic makeup, congenital disorders, senile changes, metabolic disorders, medical, physical, and environmental factors, and other pathological conditions can lead to infertility related to impaired or weak ejaculation capacity, sperm morphology, motility, and number.<sup>3,4</sup> Both reduced sperm count (oligozoospermia), and absence of sperm in semen (azoospermia) can increase the possibility of infertility in males.<sup>5</sup> Nowadays, several ART strategies such as *in vitro* fertilization, testicular sperm extraction, intracytoplasmic sperm injection, etc., along with hormone therapy (i.e. estrogen receptor modulators) and antioxidants are helpful in the restoration of the male reproduction system to have a child without satisfactory outcomes.<sup>6,7</sup> Along with these statements, development and finding therapeutic strategies are at the center of attention.<sup>8</sup>

The phenomenon of spermatogenesis is an intricate mechanism with the close collaboration of different cell lineages and the balance of sex-related hormones.<sup>9</sup> Besides, it was suggested that maintaining the balance between degradation, and bioenergetic supply has profound impacts on spermatogenesis and steroidogenesis.<sup>10</sup> In this regard, previous studies have unveiled the essential role of autophagic response in the regulation of various cell bioactivities such as the elimination of injured organelles, and misfolded proteins from the host cells. These features can influence cell homeostasis, dynamic growth activity, maturation, and differentiation.<sup>11</sup> The activation of autophagy occurs in response to various insulting, and stressful conditions and exposure of host cells to harsh microenvironments, leading to the activation of diverse downstream effectors, namely autophagy-related genes.<sup>12</sup>

Under diabetic conditions, the increase of glucose contents and byproducts can directly affect the testicular microenvironment and cell function such as Leydig, and Sertoli cells. In response to hyperglycemic conditions, the stimulation of apoptotic changes in Leydig cells can increase the possibility of structural changes in the testes.<sup>13</sup> Likewise, certain microanatomical structures such as blood-testis barrier integrity are lost following the activation of different molecular signaling pathways and accumulation of excessive free oxidant radicals.<sup>14</sup> It has been shown that adaptive autophagy can reduce the detrimental effects of several pathological conditions on the reproduction system.<sup>15</sup> However, the lack of appropriate autophagic response, or an abnormal and excessive autophagy stimulation, i.e., under diabetic conditions, can distort the homeostatic properties of testicular tissue cell functions.<sup>16</sup> Thus, the restoration of adaptive autophagy function is thought to alleviate the pathological conditions, having profound impacts on fertility beyond spermatogenesis.

In recent decades, the advent of 3D culture techniques has helped biologists to recapitulate *in vivo*-like microenvironments at the laboratory scale.<sup>17</sup> Using different 3D culture strategies such as cell aggregation, and natural and synthetic biomaterials it is possible to precisely monitor underlying molecular mechanisms in regenerative medicine area.<sup>17,18</sup> Despite these advantages in the monitoring critical role of autophagy in the process of spermatogenesis, few reports exist related to the modulation of autophagic response in 3D cultured testicular tissue units in an *in vitro* setting. Therefore, this study aimed to explore the effects of autophagy inhibition/activation on the promotion of spermatogenesis using 3D alginate-gelatin (Alg/Gel)-based hydrogels in *in vitro* conditions (**graphical abstract**). The possible effects of autophagy response, either in inhibitory or stimulatory states, were also assessed under diabetic mice.

## Materials and methods

### *Alg/Gel hydrogel synthesis protocol*

Here, in this study, Alg/Gel hydrogel was fabricated using an ionic cross-linker CaCl<sub>2</sub> according to previously published data.<sup>19</sup> In short, sodium Alg powder (I-1G, high content of guluronic acid, and MW: 70 kDa; Kimica; Japan) was sterilized using 70% EtOH solution and dissolved in calcium-free Krebs Ringer HEPES-buffered saline with adjusted pH of 7.4. Gel (CAS 9000-70-8; Sigma-Aldrich) was sterilized using chloroform at 4°C. The mixture of Alg and Gel was prepared by adding Gel to the Alg solution to create a hydrogel with concentrations of 1% w/v for both Alg and Gel. The procedure continued with the addition of 0.2 M CaCl<sub>2</sub> to facilitate the cross-linking of Alg and Gel.

### ***Physicochemical properties***

#### ***Fourier-transform infrared spectroscopy (FTIR)***

ATR-FTIR spectroscopy was used to monitor the chemical structure of Alg/Gel hydrogel and the efficiency of the synthesis protocol based on the standard protocols.<sup>20</sup> In brief, Alg/Gel hydrogel (n=3) was frozen at -20°C and immediately lyophilized. The attenuated total reflectance technique of the ATR-FTIR spectrum of Alg/Gel hydrogel was analyzed by a Varian 610 spectrometer, with a DTGS detector and a diamond crystal.

#### ***Degradation rate***

This assay evaluates the degradation and destruction of hydrogels in the target aqueous phases.<sup>21</sup> Alg/Gel hydrogels were synthesized in cylindrical molds (1 x 1 x 1 cm), and placed in a normal saline solution at 37°C for 11 days. Samples were collected on days 0, 4, 7, and 11, and their weights were recorded (W<sub>0</sub>). The samples were then stored at -20°C and later lyophilized. After lyophilization, the weights were measured again (W<sub>1</sub>) (n=4). The degree of weight loss was calculated using the following equation with four replicates.

(1)

$$\text{Weight loss \%} = \frac{(W_1 - W_0)}{W_0} \times 100$$

#### ***Swelling ratio***

The swelling capacity of Alg/Gel hydrogel was monitored after being incubated in phosphate-buffered saline (PBS) at 37°C. On various time intervals including, 1, 6, 12, 24, 48, and 72 hours, samples were taken and weighed after removing the surface water using filter papers (n=4).<sup>22</sup> The swelling ratio was calculated using the below equation, where W<sub>0</sub> and W<sub>1</sub> are the initial and swelled weights of the hydrogels respectively at different time points. This assay was performed in triplicate.

$$\text{Swelling ratio \%} = \frac{(W_1 - W_0)}{W_0} \times 100 \quad (2)$$

#### ***Mechanical properties***

An extensometer instrument was applied to evaluate the mechanical pressure tolerance of fabricated Alg/Gel hydrogel. Cylindrical scaffold samples (1 x 1 x 1 cm) were synthesized and subjected to a compression rate of 2 mm per minute (n=3). The second Young's modulus was determined as the slope of a linear fit to the stress-strain curve. The relationship between stress, strain, and Young's modulus was analyzed using the following formula: *Stress = E × Strain*.

### **SEM imaging**

Hydrogels were fixed in 2.5% glutaraldehyde solution and subjected to dehydration using ascending EtOH series. Both cell-free and cell-loaded samples were gold-sputtered and the microstructure features were imaged using the FE-SEM system (Mira-3 FEG SEM microscope, Tescan Co., Czech) under an acceleration voltage of 15kV.

### **Animals and ethics**

The *in vitro* and *in vivo* phases of the present study were approved by the local ethics committee of Tabriz University of Medical Sciences (IR.TBZMED.REC.1401.280) and animals were treated according to the “Principles for the Care and Use of Laboratory Animals” (NIH, 1996). Animals were kept inside standard cages and under standard environmental conditions with free access to tap water and chewing pellets.

### **MTT assay**

To evaluate the effects of a fabricated Alg/Gel hydrogel on whole testis cells, an MTT assay was conducted. For this purpose, male Wistar rats, ranging between 20-250 g, were humanly euthanized using an overdose of Ketamine and Xylazine. Under sterile conditions, testes were sampled and transferred to the Cell Culture Lab of the Stem Cell Research Center affiliated with Tabriz University of Medical Sciences. Tissues were chopped into small pieces and then subjected to enzymatic digestion using 0.1% type I collagenase (9001-12-1, Sigma-Aldrich) for 10-20 minutes. The enzyme activity was neutralized using fetal bovine serum (FBS; Gibco) solution, and the suspended cells were passed through 200  $\mu\text{m}$  pore-sized meshes. The cells were collected, counted using a hemacytometer slide, and mixed with Alg/Gel solution ( $2 \times 10^6$  per 1 mL of hydrogel). The mixture was incubated with 200 mM  $\text{CaCl}_2$  for solidification of Alg/Gel mixture. Approximately 50  $\mu\text{L}$  of hydrogel containing  $1 \times 10^4$  cells were transferred onto each well of a 96-well plate and maintained for 7 days under standard culture conditions (37°C, 95% relative humidity, and 5%  $\text{CO}_2$ ). After the completion of the incubation period, the supernatants were discarded and replaced with 100  $\mu\text{L}$  MTT solution (2 mg/mL) and kept at 37°C for 4 hours. The procedure continued with the addition of a DMSO solution, and the OD values were measured at 590 nm using a microplate reader (Model: Elx808; BioTek). In the control group, isolated cells were plated on a hydrogel-free plastic surface for comparison with a similar initial cell density. The data were expressed as a % of the control group. The procedure was performed in 15 replicates per group.

### **Testicular organoid culture**

In this study, we developed a 3D testicular organoid culture system using Alg/Gel hydrogel. The rat testes were cut into 2 mm slices. After that, 400  $\mu\text{L}$  Alg/Gel hydrogel was poured onto each well of 24-well plates. A single testicular tissue fragment was placed in each well and the procedure was followed by overlaying an additional 400  $\mu\text{L}$  Alg/Gel hydrogel. The mixture was polymerized using a  $\text{CaCl}_2$  solution. To exclude the toxicity of excessive calcium ions, each well was washed three times using PBS. The fragments were incubated with DMEM/HG culture medium containing 10% FBS and 1% Pen-Strep solution under standard conditions for 7 days. To promote active dynamic growth and induction of spermatogenesis cultured testicular organoids, 10  $\mu\text{M}$  testosterone (Aburaihan Pharmaceutical Co.), 5  $\mu\text{M}$  retinoic acid (Cas No: 302-79-4, Sigma-Aldrich), and 100 ng/mL rFSH (CinnaGen; Tehran; Iran) were added into the culture medium.<sup>23</sup> The culture medium was replenished every 3-4 days. This procedure was performed in triplicates per group.

### ***Modulation of autophagy response***

To this end, testicular organoids within the Alg/Gel hydrogel were exposed to 5  $\mu$ M metformin (Met; Osvah Pharmaceutical Co.; Tehran; Iran), or 15  $\mu$ M hydroxychloroquine (HCQ; Cat No: H0915, Sigma-Aldrich) to modulate the autophagy response.<sup>24-26</sup> The culture medium was renewed every 3-4 days and organoids were kept under standard culture conditions for 7 days.

### ***Western blotting***

After 7-day culture time, incorporated testicular organoids were removed from supporting Alg/Gel hydrogel after 5 minutes using 0.1 M sodium citrate followed by washing steps (3X).<sup>27</sup> Organoid masses were lysed using protein lysis buffer [0.1% SDS, 150 mM NaCl, 50 mM Tris HCl, 1% NP-40, 2 mM EDTA] overnight at 4°C. The lysates were centrifuged at 11,000 rpm for 20 minutes at 4°C. Protein contents were measured using BCA assay, and 10  $\mu$ g protein from each group was electrophoresed on 10% SDS-PAGE gel. After transferring onto the PVDF membranes, a panel antibody including anti-human Beclin-1 (Cat no: sc-48341; Santa Cruz Biotechnology, Inc.), LC3 (Cat no: Sc-398822; Santa Cruz Biotechnology, Inc.), and P62 (Cat no: Sc-10117; Santa Cruz Biotechnology) was used to monitor autophagy effectors. Membranes were incubated with primary antibodies overnight at 4°C. After three PBS washes, HRP-tagged secondary antibodies (Cat no: sc-2357, Santa Cruz Biotechnology, Inc.) were used for labeling of immunoreactive bands on X-ray films after the addition of ECL solution. Using ImageJ software (ver.1.4; NIH), the density of each immunoreactive band was calculated. The values were expressed as relative protein levels compared to housekeeping protein  $\beta$ -actin (Cat no: sc-517582; Santa Cruz Biotechnology, Inc.). This procedure was performed in triplicate for each protein tested.

### ***H & E staining***

The tissue structure and further microstructure changes were monitored using H & E staining. On day 7, organoid-laden Alg/Gel hydrogels were gently removed and fixed using a 10% buffered formalin solution. After passing dehydration, and rehydration steps, the paraffin-embedded samples were cut into 5  $\mu$ m-thick slices and stained using H & E solution. Three sections per sample were prepared, and the entire section was evaluated for histopathological assessments. To analyze the cellular population within the seminiferous tubules, over 20 high-power fields were randomly selected, and the cells in different developmental stages were noted. WHO guidelines were implemented to annotate cells at various stages within the seminiferous tubules.

### ***Immunofluorescence (IF) staining***

To monitor the influencing effects of autophagy on the density of tissue progenitor cells in testicular organoids, IF staining was performed in terms of Oct3/4<sup>+</sup> cells (n=3 per group).<sup>28</sup> Organoid-laden Alg/Gel hydrogels were incubated with OCT compound, and snap-frozen at -20°C. Using the cryosection technique, 5  $\mu$ m-thick slices were prepared. In the next step, samples were allowed to be thawed and washed three times with PBS. Then, samples were treated with 0.5% Triton X-100 for 5 minutes to permeabilize the cell membrane. The procedure was continued with the blocking of samples using 1% FBS for 5-10 minutes and anti-Oct3/4 antibody (Dilution: 1: 500; Cat no: sc-5279; Santa Cruz Biotechnology, Inc.) overnight at 4°C. Afterward, samples were washed three times with PBST (3  $\times$  10 minutes) and incubated with FITC-conjugated secondary antibody (Cat no: sc-2010; Santa Cruz Biotechnology, Inc.) for 1 hour at RT. After three PBST washes, DAPI (1  $\mu$ g/ml; Sigma-Aldrich) was used for nuclear staining. Samples were imaged using a fluorescence microscope (Model: BX41; Olympus; Japan).

### *Oxidative stress status*

The oxidative status of oxidative status in testicular organoid-loaded Alg/Gel hydrogel was also studied after treatment with 5  $\mu$ M Met or 15  $\mu$ M HCQ. The protein lysates were used for measuring glutathione peroxidase (GPx; RANDOX Laboratories), superoxide dismutase (SOD; RANDOX Laboratories Ltd), and total antioxidant capacity (TAC; RANDOX Laboratories) levels according to the manufacturer's instruction. This procedure was performed in triplicates per group.

### *Induction of diabetes mellitus (DM)*

Fifteen BALB/c male mice, ranging from 25-30 g, were randomly selected for induction of long-lasting DM using streptozotocin (STZ; Cat no: S0130; Sigma Aldrich).<sup>29</sup> The recommended dose was dissolved in solution containing same volume of sodium citrate (2.94 g/100 ml; Sigma-Aldrich) and citric acid (2.1 g/100 ml water; Sigma-Aldrich) solution (pH =4.5). STZ at a dose of 50 mg/kg body weight was administered in three separate injections via an intraperitoneal route with an average interval of 2 days. Four days after the last injection, the systemic levels of glucose were monitored using a glucometer (Model: TD-4277; Aktivmed GlucoCheck XL). Levels of more than 250 mg/dL were conceived as diabetic conditions.

### *Effect of Met and HCQ in testicular tissue of diabetic mice*

Mice were randomly divided into three groups (each in 5) as follows; non-treated Control, DM, DM + Met, and DM + HCQ groups. In DM + Met mice, 120 mg/kg of body weight Met was injected via i.p. once per week for 4 weeks into the DM mice. This protocol was implemented to investigate the effects of sustained, long-term modulation rather than acute daily fluctuations. In the DM + HCQ group, the DM mice received 70 mg/kg body weight HCQ once a week for 4 weeks. Distilled water (DW) was used as a vehicle for all injections. In the control mice, DW alone was used as the control vehicle. Additionally, animals were monitored daily for clinical signs of toxicity and weight loss, and no adverse effects were observed. One week after the last injection, the mice were euthanized using an overdose of ketamine, and xylazine, and epididymis was used for the analysis of sperm parameters. Testes were fixed inside a 10% buffered formalin solution and subjected to H & E staining as above-mentioned. For histological examination, the number of spermatogonial cells, spermatocytes, and spermatids were counted in each seminiferous tubule in slides. The spermogram analysis was conducted in a blinded manner according to WHO guidelines, using epididymal semen to assess parameters such as total sperm count, abnormalities, and motility rates (%) (n=5).

### *Statistical analysis*

Data (Mean  $\pm$  SD) were analyzed using GraphPad Prism software (ver. 8.4.3.). Student t-tests and ANOVA Tukey's post hoc test were applied to find any statistical differences between the experimental groups.  $p < 0.05$  was used to describe the existence of significant differences between the groups.

## **Results and Discussion**

### **Alg/Gel hydrogel physicochemical properties**

#### **FTIR**

Using FT-IR spectra of Gel, Alg, and Alg/Gel hydrogel, the chemical structures were monitored (**Figure 1A**). Based on data, Alg alone exhibits two characteristic absorption bands at 1617  $\text{cm}^{-1}$  and 1418  $\text{cm}^{-1}$  and is attributed to the asymmetric and symmetric stretching vibration of the -COO group, respectively. An adsorption

band at  $3446\text{ cm}^{-1}$  is related to the stretching vibration of the hydroxyl functional group and a stretching vibration absorption peak of the  $-\text{CH}_2$  group at  $2926\text{ cm}^{-1}$ .<sup>30</sup> The characteristic absorption bands of gelatin at  $1648\text{ cm}^{-1}$ ,  $1540\text{ cm}^{-1}$ , and  $1238\text{ cm}^{-1}$  were attributed to amide I (C=O and C-N stretching), amide II and amide III (mainly N-H bending, and C-N stretching vibration), respectively. Finally, the wide absorption band around  $3421\text{ cm}^{-1}$  was due to the N-H stretching vibration.<sup>31</sup> From the FT-IR spectra of Alg/Gel hydrogel, it was indicated that the characteristic strong absorption band at  $1648\text{ cm}^{-1}$  (amide I) of Gel shifted to a lower wave number at  $1637\text{ cm}^{-1}$  and indicated the interaction between Gel amino and Alg carboxylic groups (**Figure 1A**). Moreover, the slight shift of the peak of amide I from  $1647\text{ cm}^{-1}$  to  $1637\text{ cm}^{-1}$  in the Alg/Gel composite confirms the fact that negative groups of Alg can interact with positively charged groups of Gel.<sup>32</sup> The peak at  $1261\text{ cm}^{-1}$  (amide III) indicates the presence of Gel in the final composite. At the same time, the absorption  $-\text{NH}$  band of Gel at about  $3421\text{ cm}^{-1}$  and  $-\text{OH}$  band of Alg at about  $3421\text{ cm}^{-1}$  broadened and shifted to a lower wave number at  $3417\text{ cm}^{-1}$ , suggesting an increase in the hydrogen bonding (**Figure 1A**).<sup>32,33</sup> All those changes show strong evidence of the intermolecular interactions between  $-\text{OH}$  groups of Alg and  $-\text{NH}$  groups of Gel molecules.

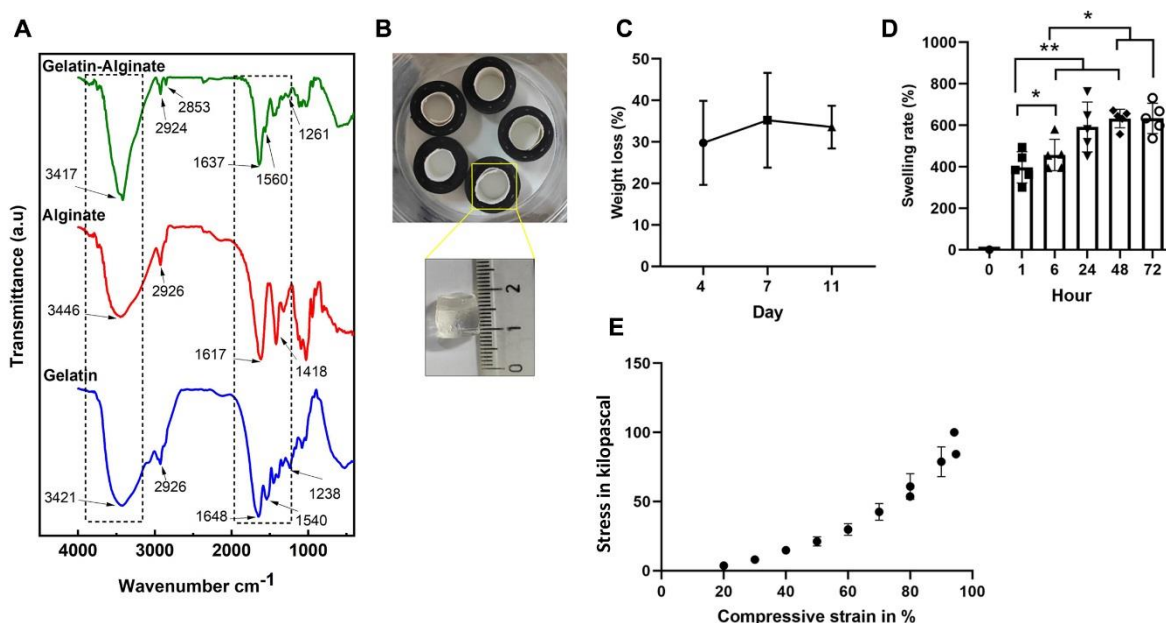


**Figure 1.** FTIR analysis of Alg/Gel composite after ionic cross-linking using  $\text{CaCl}_2$  (A;  $n=4$ ). The suspension of Alg/Gel hydrogel was cast using cylindric models followed by the addition of 200 mM  $\text{CaCl}_2$  for ionic cross-linking (B). Monitoring degradation rate (C;  $n=4$ ), Swelling ratio (D;  $n=4$ ), and mechanical properties (E;  $n=3$ ). All quantified data are presented as mean  $\pm$  SD.

### Biodegradation, swelling, mechanical properties

In this study, Alg/Gel hydrogel masses were fabricated using cylindric molds for assessing physicochemical properties (**Figure 1B**). Biodegradation analysis revealed 30% weight loss in the first 4 days, and these values reached 35% on day 7 (**Figure 1C**). Based on our findings, the incubation of Alg/Gel hydrogel in the aqueous phase for 11 days can contribute to 33% weight loss (**Figure 1C**). Taken together, it can be told that the existence of degradation in fabricated Alg/Gel hydrogels makes them responsive to the biological fluids, and replacing with the natural matrix over time.

Data confirmed the swelling capacity and ability to absorb water over 72 hours (**Figure 1D**). We noted that Alg/Gel hydrogels show an upward trend in weight gain after 1, 6, 24, and 48 hours. Also, the water absorption capacity of Alg/Gel substrates was relatively constant after 48 hours in which no statistically significant differences were achieved in terms of swelling ratio at time points 48 and 72 hours ( $p>0.05$ ; **Figure 1D**). According to the obtained data, the fabricated Alg/Gel hydrogel scaffold exhibited relatively appropriate resistance to mechanical pressure (**Figure 1E**). The samples measured in three repetitions were broken at an average strain of about 89.70%. Also, the ultimate compressive strength (UCS) was evaluated as 45.97 Kilopascal on average (**Figure 1E**).

### SEM imaging

SEM images the existence of pores within the Alg/Gel hydrogel (**Figure 2A-B**). Based on our estimation, the average size of pores reached  $36.28 \pm 13.61 \mu\text{m}$  (**Figure 2B**). These data show the existence of a porous structure within the fabricated Alg/Gel hydrogel. Further analysis indicated the attached cells inside the polymeric network with the acquisition of flattened morphologies. These features support the notion that Alg/Gel hydrogel provides a suitable platform for attachment and suitable morphology of incorporated cells (**Figure 2C**).

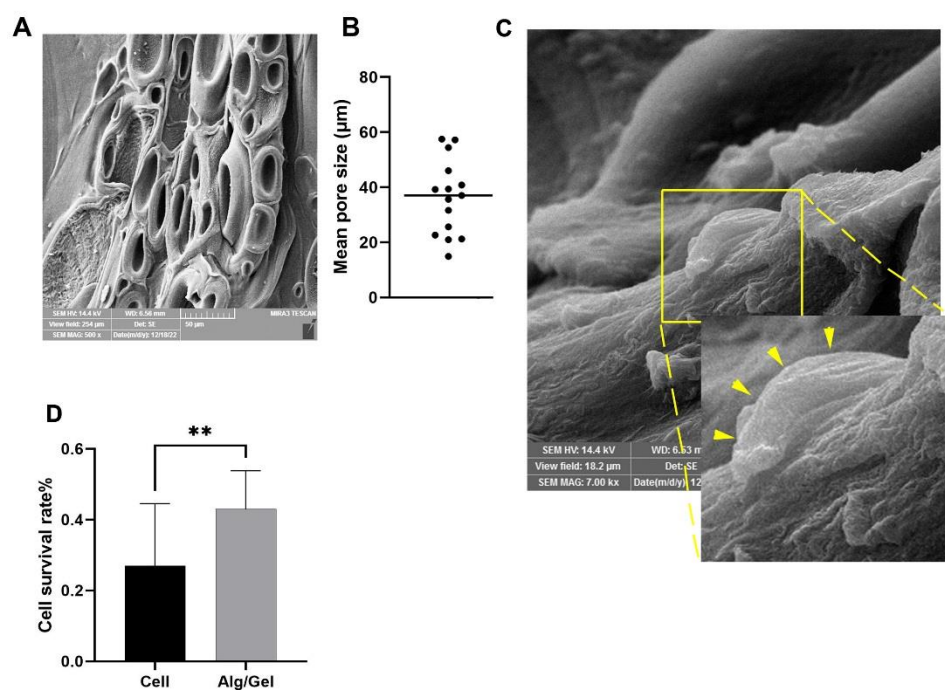


**Figure 2.** SEM analysis of Alg/Gel hydrogel porosity (**A**), and cell adhesion (**B**). The yellow arrowheads indicate flattened cell mass adhered tightly to the Alg/Gel surface after 7 days of culture in *in vitro* conditions (**C**). Monitoring the survival rate of whole testicular tissue cells after 7 days plated on Alg/Gel hydrogel compared to control cells cultured on a plastic surface (**D**;  $n=15$ ). Student t-test.  $**p<0.01$ . All quantified data are presented as mean  $\pm$  SD.

### Alg/Gel substrate induced survival rate of testis cells

Conventional MTT assay indicated that a 7-day culture of freshly isolated testis cells led to an enhanced survival rate when compared to the control group ( $p<0.01$ ; **Figure 2D**). These features show that Alg/Gel hydrogel provides a suitable microenvironment for the induction of viability of testis cells.

**Autophagy modulation in testicular organoids**

The autophagic response was monitored in Met, and HCQ-treated testicular organoid-loaded Alg/Gel hydrogels after 7 days *in vitro* (**Figure 3A-B**). Data indicated the statically significant increase of Beclin-1, LC3-II/I ratio coincided with a reduction of P62 in Met-treated groups compared to non-treated control, and HCQ groups ( $p < 0.05$ ). These data indicate that Met can stimulate the autophagic response in the early steps (Beclin-1 $\uparrow$ ), while the increase of LC3-II/I ratio and total LC3 levels are indicative of enhanced autophagy flux. The reduction of P62 confirms the completion of autophagic response (**Figure 3A-B**). On the contrary, the addition of HCQ can blunt the autophagy signaling pathway in which an inverse pattern was evident as compared to the Met-treated group ( $p < 0.05$ ; **Figure 3A-B**). Compared to the control group, protein levels of Beclin-1, and P62 except for total LC3 content remained unchanged in the HCQ-treated group. Thus, we noted that HCQ can blunt the autophagic response in testicular organoid-loaded Alg/Gel hydrogels via the regulation of autophagic flux. Taken together, data from western blotting confirmed the influencing impacts of Met and HCQ on the autophagy signaling pathway in the 3D cultured testicular tissue fragments after 7 days *in vitro*.

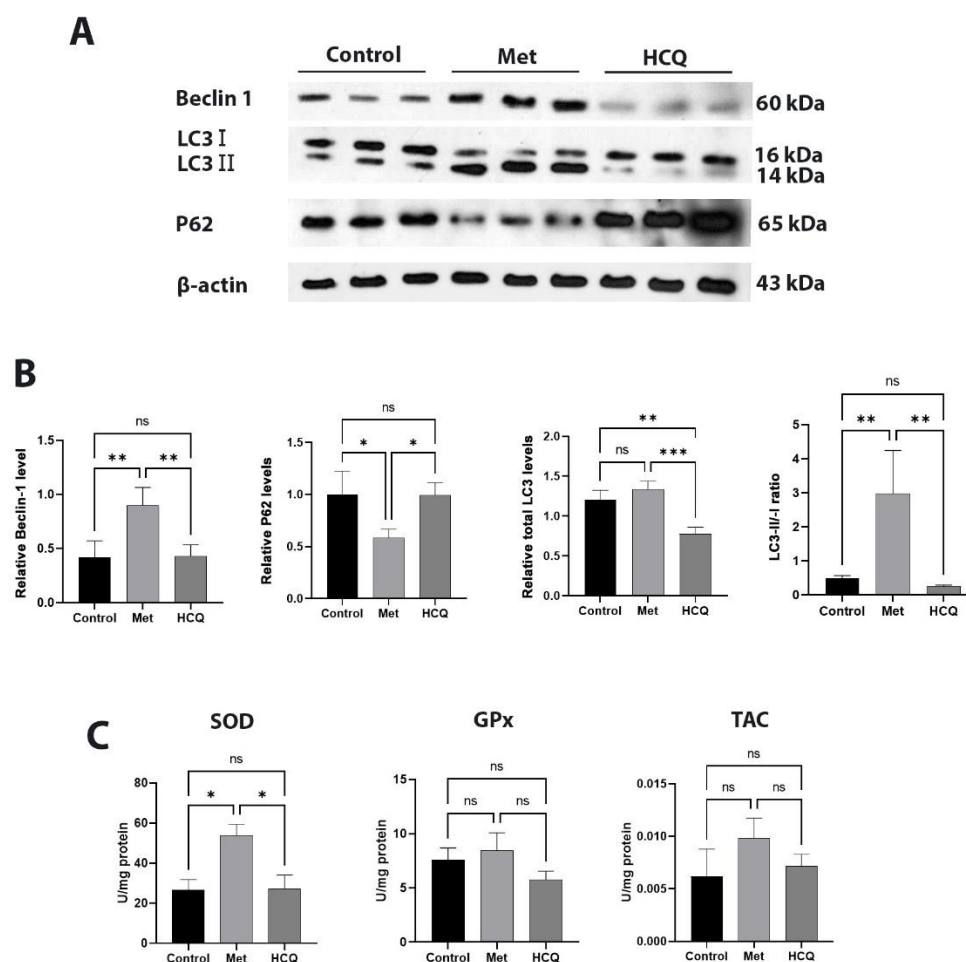


**Figure 3.** Monitoring the autophagy-related protein levels using western blotting in rat testicular organoids encapsulated inside Alg/Gel hydrogel in response to 5  $\mu$ M Met and/or 15  $\mu$ M HCQ after 7 days (**A** and **B**;  $n=3$ ). Each column represents the average (mean  $\pm$  SD) of three biological replicates normalized with  $\beta$ -actin as a loading control (**B**). Data indicated the stimulation and inhibition of autophagy response via the alteration of Beclin-1, total LC3 levels, LC3-II/I ratio, and P62 in organoid mass compared to the control organoids. The antioxidant capacity of rat testicular organoids was also assessed in terms of SOD, GPx, and TAC after 7 days in Met- and HCQ-treated groups (**C**;  $n=3$ ). Data confirmed an activated SOD status and a slight increase in GPx function and TAC levels in the presence of Met but not HCQ. One-way ANOVA with Tukey post hoc analysis. \* $p < 0.05$ ; \*\* $p < 0.01$ ; \*\*\* $p < 0.001$ . All quantified data are presented as mean  $\pm$  SD.

**Antioxidant properties were enhanced in the Met-treated testicular organoids**

Data revealed an increased SOD activity in the presence of Met compared to the control and HCQ-treated groups ( $p < 0.05$ ; **Figure 3C**). Non-significant differences were found in terms of GPx, and TAC between the groups. Even though, treatment of encapsulated organoids with Met and/or HCQ did not alter the activity of GPx, and TAC in comparison with the non-treated organoids ( $p > 0.05$ ; **Figure 3C**). Therefore, one can hypothesize that the stimulation of autophagy response can recruit the activity of an early-stage antioxidant enzyme SOD in encapsulated testicular organoids within the Alg/Gel hydrogel after 7 days.

**Autophagy modulation altered the maturation of sperm cells in testicular organoids**

H & E staining was used to follow up any histological changes in testicular organoids in the presence of Met, and/or HCQ after 7 days within the Alg/Gel hydrogel (**Figure 4A-B**). In the non-treated control group, sperm cells at different developmental stages, both spermatocytes and spermatids, were detected. Bright-field images showed that the number of nucleated cells was reduced in the Met-treated organoids while these changes were less in the HCQ group (**Figure 4A**). Along with these changes, sperm cell counting revealed the reduction of maturing cells like spermatids and spermatocytes in the lumen of seminiferous tubules in the Met-treated organoids compared to the control and HCQ groups ( $p < 0.001$ ; **Figure 4B**). Notably, autophagy inhibition using HCQ did not yield statistically significant differences in terms of maturing sperm cells compared to the control organoids ( $p > 0.05$ ).

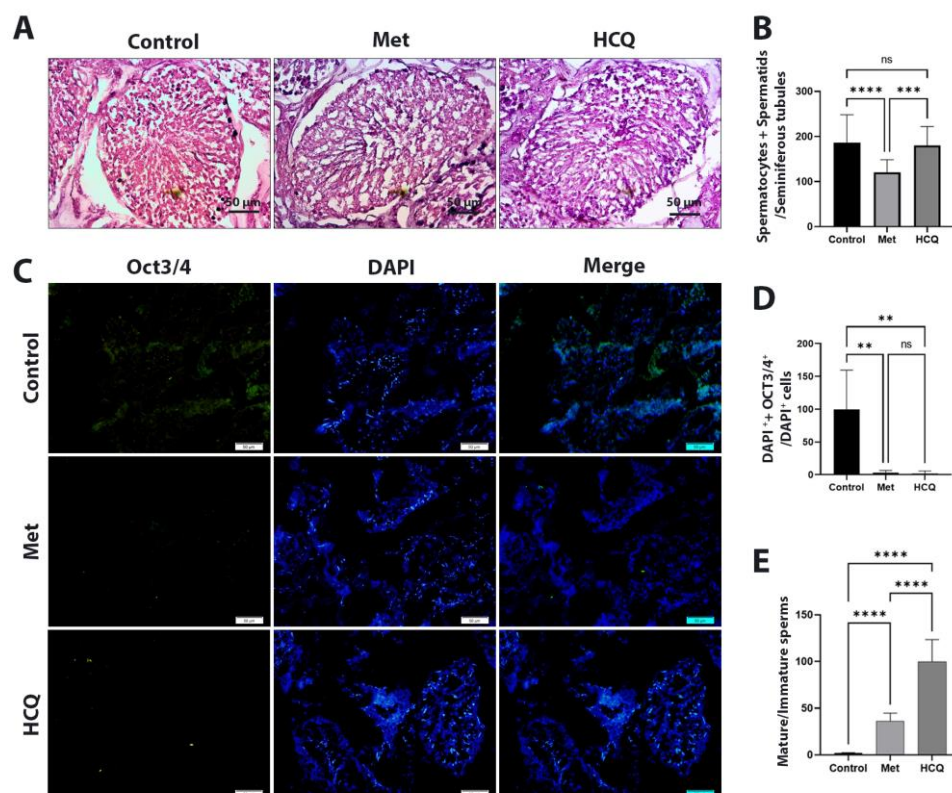


**Figure 4.** Histological examination (H & E staining) of rat testicular organoids within the Alg/Gel hydrogel after treatment with Met, and HCQ (**A-B**;  $n=20$ ). Data indicated the alteration of immature sperm cells per seminiferous tubules within the organoids after 7 days related to non-treated organoids. Monitoring the density of OCT3/4<sup>+</sup> progenitors inside organoids seminiferous tubules in Met-, and HCQ-treated organoids (**C**, **D**, and **E**;  $n=4$ ). Data indicated the reduction of OCT3/4<sup>+</sup> progenitors and an increase of maturing sperm cells in treated organoids. Scale bar=50  $\mu$ m. One-way ANOVA with Tukey post hoc analysis. \*\* $p < 0.01$ ; \*\*\* $p < 0.001$ ; and \*\*\*\* $p < 0.0001$ . All quantified data are presented as mean  $\pm$  SD.

In parallel with H & E staining, the density of OCT3/4<sup>+</sup> spermatogonial stem cells per seminiferous tubules was also determined using IF staining (**Figure 4C-E**). Based on the present data, the number of OCT3/4<sup>+</sup> spermatogonial stem cells was significantly declined in Met-, and HCQ-treated organoids compared to the control group ( $p < 0.01$ ; **Figure 4C-D**). The OCT3/4<sup>+</sup>/OCT3/4<sup>-</sup> ratio was also calculated to predict the maturation capacity of sperm cells in the presence of Met, and/or HCQ (**Figure 4E**). The results indicated a significant increase in the ratio of mature to immature cells (OCT3/4<sup>-</sup>/OCT3/4<sup>+</sup>) ratio in the Met and HCQ groups compared to control organoids ( $p < 0.0001$ ). Besides, the incubation of testicular organoids with HCQ had more significant effects on increased sperm cell maturation (OCT3/4<sup>-</sup>/OCT3/4<sup>+</sup>) related to the Met-treated group ( $p < 0.0001$ ; **Figure 4E**). These data indicate that modulating autophagy can influence the regenerative potential of rat testes by regulating the early signs of differentiation in sperm cells.

#### Autophagy can alter sperm cell number and dynamic growth in diabetic mice

Our findings revealed that both Met and HCQ treatments have suppressed the number of spermatogonial, spermatocyte, and spermatid cells within the seminiferous tubules (**Figure 5A-B**). Despite the existence of this pattern, non-significant differences were achieved in some sperm cell subsets. Besides, DM can significantly decrease sperm cells in all the developmental stages with a notable decline in the spermatogonial and spermatid cells ( $p < 0.0001$ ; **Figure 5A-B**). The administration of Met and HCQ for 4 weeks ameliorated the diabetic condition in terms of sperm cell counts, however, these changes were not statistically significant as compared to the diabetic state ( $p > 0.05$ ; **Figure 5A-B**).

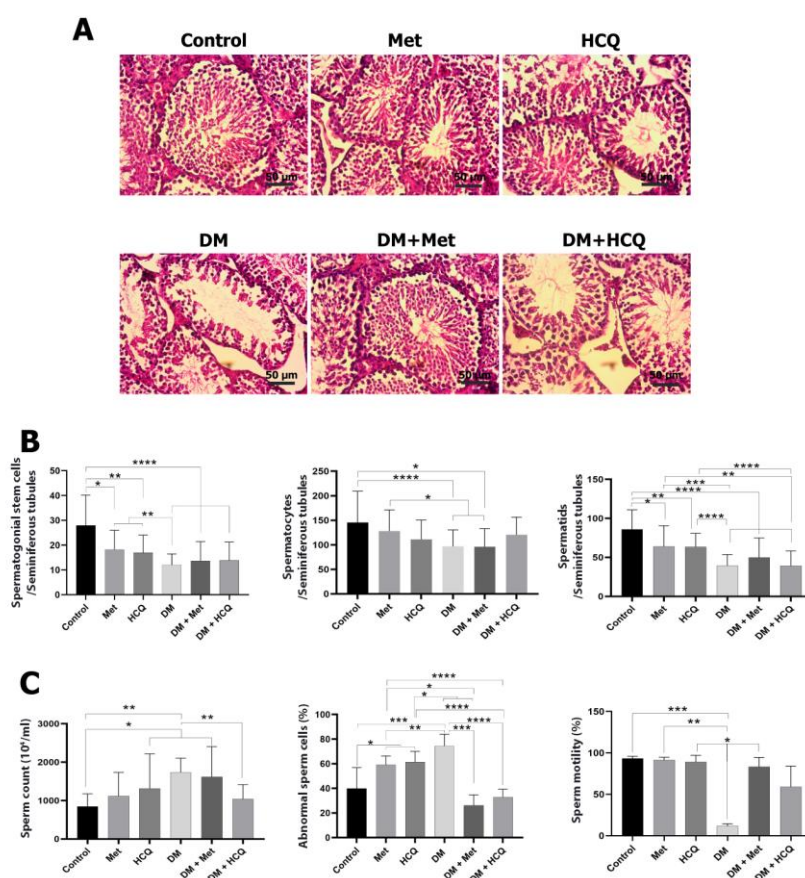


**Figure 5.** Monitoring histological changes in murine testicular tissue under diabetic conditions after receiving Met and/or HCQ (**A-B**). Spermogram analysis of semen samples from different groups (**C**;  $n=5$ ). Data indicated the improvement of some sperm parameters in diabetic mice after administration of Met, but not HCQ after 4 weeks. Scale bar=50  $\mu$ m. One-way ANOVA with Tukey post hoc analysis. \* $p < 0.05$ ; \*\* $p < 0.01$ ; \*\*\* $p < 0.001$ ; and \*\*\*\* $p < 0.0001$ . All quantified data are presented as mean  $\pm$  SD.

We also noted that DM influenced the murine sperm parameters in terms of count abnormality and motility (**Figure 5C**). A significant increase in the number of sperms, higher rates of abnormality, and the lowest percentage of motility were indicated under diabetic conditions ( $p < 0.05$ ; **Figure 5C**). Interestingly, it was noted that inhibition of autophagy in diabetic mice (DM+HCQ) resulted in a decline in the number of sperm cells compared to the matched control DM group ( $p < 0.01$ ) and closed it to the basal control levels. In DM + Met, and DM + HCQ groups, the percentage of sperms with normal morphology and motility increased ( $p < 0.001$ ; **Figure 5C**). Interestingly, Met and HCQ administration increased sperm counts and raised the percentage of abnormal sperm in non-diabetic conditions ( $p < 0.05$ ). We found a non-significant difference in terms of sperm motility in DM mice after receiving Met and/or HCQ ( $p > 0.05$ ; **Figure 5C**). These data support the notion that autophagy modulation, either stimulation or inhibition, can alter some sperm parameters in diabetic mice.

## Discussion

This study was carried out to investigate the effect of autophagy on dynamic growth and regenerative potential of rat testicular organoids within the Alg/Gel hydrogel in response to autophagy stimulation/inhibition. How and by which mechanism autophagy modulation can affect the process of spermatogenesis was also monitored in diabetic mice.

Data confirmed suitable physical and chemical properties indicated the successful ionic cross-linking between the Alg and Gel. For example, the degradation of Alg/Gel hydrogel initiated significantly after 4 days and reached a relatively steady state. Inside the body, the replacement of calcium ions with sodium ions can lead to the absorption of water molecules and the loosening of the polymeric network.<sup>34</sup> With the initiation of degradation, the possibility of natural ECM production increases after being transplanted into the target sites.<sup>35,36</sup> Having an interconnected porous microenvironment with an average pore size of  $36.28 \pm 13.61 \mu\text{m}$ , the migration of transplanted cells, and/or host tissue is facilitated into the deeper layer of hydrogel.<sup>37</sup> This feature allows suitable penetration of nutrients and drainage of cell byproducts while immune cells can recruit the Alg-based grafts, leading to replacement with natural ECM at appropriate times.<sup>38</sup> MTT data indicated an enhanced survival rate in cultured whole testicular tissue cells compared to the cells cultured on plastic surfaces. It was suggested the existence of 3D polymeric networks with several motifs in the structure Gel, a denatured collagen form, improves cultured cell attachment and phenotype acquisition.<sup>27,39</sup> According to these data, natural hydrogels composed of Alg plus Gel are suitable for the expansion of different testicular tissue cells.

It was noted that the addition of  $5 \mu\text{M}$  Met, and  $15 \mu\text{M}$  HCQ can efficiently stimulate, and inhibit the autophagic response in testicular organoids encapsulated within the Alg/Gel hydrogel. It has been indicated that Met can boost the autophagic response by increasing protein levels of Beclin-1, LC3-II/-I ratio, and reduction of P62 in different tissues such as the liver.<sup>40</sup> The increase in total LC3 contents along with the conversion into LC3-II indicated lipidation and an increase of autophagosome formation. In later steps, these autophagosomes are directed toward lysosomes to form autophagolysosomes which further recycle the biomolecules or excrete them out of host cells.<sup>41</sup> We also found that HCQ, an autophagy inhibitor, exerts opposite effects on testicular organoids after 7 days. The increase of P62 in the presence of HCQ indicated blockade of autophagic flux coincided with the accumulation of autophagosomes, and an incomplete autophagy response.<sup>42</sup> It has been thought that excessive intracellular autophagolysosomes can contribute to a delay in the secretion of misfolded proteins and damaged organelles, making cells sensitive to different insulting conditions.<sup>43</sup> These features indicate the success of the current protocol in the stimulation and inhibition of autophagy response inside the testicular organoids. The significant increase of SOD, and slight changes in TAC, and GPx activity in Met-treated organoids would be

related to the fact that activation of autophagy can scavenge harmful free radicals during the culture of testicular organoids.<sup>44</sup> Even though, the inhibition of autophagy using HCQ did not alter the activity of anti-oxidant enzymes related to the control conditions. As a common belief, HCQ can increase intracellular contents of reactive free radicals by the inhibition of autophagy response.<sup>45</sup> However, the dose of HCQ used in current protocol was not at a level that causes oxidative stress as compared to the control levels.

Emerging data have confirmed the putative effects of autophagy in the regulation of various cell bioactivities and differentiation potential under different biological conditions.<sup>46,47</sup> We noted that Met and HCQ change key autophagy markers, but our data doesn't show how that happens inside the cell. The most logical place to look next is the central signaling hub that controls autophagy. It's well known that metformin can switch on AMPK. One of AMPK's main jobs is to turn off mTOR, which acts as a major stop signal for autophagy. With mTOR off, the green light is given to ULK1 to start building autophagosomes.<sup>48</sup> We think this AMPK-mTOR-ULK1 chain reaction is probably how metformin works in our organoids. HCQ, on the other hand, doesn't stop the start of autophagy—it blocks the very end. It makes lysosomes less acidic so they can't properly fuse with and digest the autophagosomes, causing everything to back up. Pinpointing this sequence—whether with phospho-antibodies or direct flux tests—is the critical missing link between our treatments and the cellular changes we observed.

Histological examination indicated that treatment with autophagy activator (Met), and inhibitor (HCQ) led to the reduction of OCT3/4<sup>+</sup> progenitors spermatogenic tubes of cultured organoids after 7 days. Despite the reduction of OCT3/4<sup>+</sup> progenitors in Met, the number of maturing sperm cells such as spermatids, and spermatocytes was also reduced, indicating a diminishing cell population inside the seminiferous tubules. Considering the differences in the mode of action of HCQ, and Met, it seems that the reduction of OCT3/4<sup>+</sup> progenitors, and maturing sperm cells can be promoted by engaging distinct effectors in both groups. For example, it was shown that in response to HCQ treatment, it was shown that the number of degenerated spermatocytes, and spermatogenic cell sloughing increased simultaneously with the cell cycle arrest and interstitial edema of rat testes.<sup>49</sup> These features can promote the sloughing of all sperm cells and degenerative changes in spermatogonial stem cells as well. On the contrary, emerging data have proven the stimulatory effects of Met on sperm parameters such as motility, lactate production, acrosome reaction, etc.<sup>50</sup> It seems that the reduction of OCT3/4<sup>+</sup> progenitors is possibly related to the accelerated differentiation of these cells to maturing sperm cells.<sup>51</sup> The significant activation of SOD in Met-treated organoids indicates the increase of basal reactive oxygen species and active mitochondrial function.<sup>52</sup> The promotion of mitochondrial function and mitophagy in the presence of Met can expedite the differentiation of OCT3/4<sup>+</sup> progenitors into the maturing sperm cells. Besides, the cytoskeletal remodeling is stimulated when the degradation of PDLIM1 is increased via autophagolysosomes under autophagic response, leading to the differentiation of spermatids.<sup>53</sup>

It was found that excessive glucose levels can reduce sperm counts coincided with the increase of abnormal sperm features. This phenomenon is mainly due to the direct toxic effects of hyperglycemia on germ cells and the elimination of germinal layer seminiferous tubules.<sup>54</sup> Besides, the reduction of steroidogenesis and the reduction of testicular matrix supporting cells such as Leydig cells can exacerbate DM-related pathologies.<sup>55,56</sup> Like previously published reports, we indicated that the administration of Met in diabetic mice can restore sperm number, and motility while reducing the abnormal sperm counts.<sup>57</sup> Met did not influence the number of progenitor cells within the seminiferous tubules. Also, the reduction of spermatogonial cells in the met and HCQ groups is completely consistent with the results of the previous stages and indicates the progression of cells towards mature cells. It seems that the therapeutic effects of Met on diabetic mice spermatogenesis can be related to different

mechanisms. For example, it was shown that Met can improve testicular steroidogenesis and spermatogenesis via the expression of luteinizing hormone/chorionic gonadotropin receptors in diabetic rats.<sup>58</sup> It should not be forgotten that adaptive autophagy response is inhibited in the testicular tissue of diabetic rodents, leading to reticulum endoplasmic injury.<sup>59</sup> Thus, the stimulation of autophagy to normal levels can be an efficient strategy in diabetic conditions. Of course, caution should be taken that overactivation of autophagy not only does not restore spermatogenesis properties but also can exacerbate impaired spermatogenesis. For instance, it was indicated that the excessive autophagy response in high-fed diet mice diminished spermatogenesis potential and administration of chloroquine can blunt decreased fertility in obese, subfertile male mice.<sup>60</sup> These data indicate the dual activity of autophagy in terms of spermatogenesis potential. Notably, the autophagic response is usually impaired or aborted under prolonged hyperglycemic conditions.<sup>61</sup> Thus, activation of autophagy signaling pathway can be likely efficient in the restoration of spermatogenesis. Several aspects of our experimental design point to necessary future work. We used single doses and a single time point, so defining optimal treatment windows through detailed time-course and dose-response studies is essential. Our reliance on drug effects also means we lack genetic proof; using knockout models or lineage tracing would solidify the link between autophagy and specific germ cell fates. Furthermore, we inferred autophagic activity from protein markers. Direct flux measurements *in vivo*, alongside analysis of key hormones like testosterone and LH, would more firmly connect our treatments to testicular function. Finally, the unexpected increase in abnormal sperm in normal mice treated with either drug hints at complex effects on a balanced system, meriting a closer look in future studies. Addressing these points will be crucial to move from these promising morphological observations to a precise molecular and physiological understanding.

## Conclusion

The current study aimed to study the possible effects of autophagy response on spermatogenesis capacity in rat testicular organoids incorporated into Alg/Gel hydrogel and diabetic mice. It was shown that autophagy modulation, either inhibition or stimulation, can alter spermatogenesis potential in terms of progenitor cell density, sperm counts, and parameters. Likewise, autophagy modulation in diabetic mice using Met had profound impacts on some sperm parameters and closed them to the control levels. Data from the present study indicate that the activation of adaptive autophagy response under diabetic conditions can in part but not completely restore testicular tissue function. Whether the inhibition and/or stimulation of autophagic response can exert therapeutic outcomes needs further investigation, as autophagy can act as dual swords in terms of cell biology. Taken together, under controlled conditions autophagy stimulation can be possibly a strategic medication in diabetic individuals.

## Acknowledgments

Authors wish to thank the personnel of the Stem Cell Research Center and Core Research Laboratory, Tabriz University of Medical Sciences for their help and guidance.

## Authors' contribution

Conceptualization: Mahdi Mahdipour, Farah Farokhi

Data curation: Shadi Atazadeh

Formal analysis: Shadi Atazadeh

Investigation: Shadi Atazadeh, Maryam Hasan Sadeh

Methodology: Shahin Ahmadian, Sepideh Saghati, Fereshteh Valipour, Amir Fattahi

Project administration: Reza Rahbarghazi, Mahdi Mahdipour

Resources: Mahdi Mahdipour

Software: Shadi Atazadeh, Mahdi Mahdipour  
Supervision: Reza Rahbarghazi, Farah Farokhi, Mahdi Mahdipour  
Validation: Reza Rahbarghazi, Mahdi Mahdipour  
Writing–original draft: Shadi Atazadeh  
Writing–review & editing: Reza Rahbarghazi, Mahdi Mahdipour

### Competing interests

The authors declare no competing interests.

### Data Availability Statement

All data that support our findings in this study are available from the corresponding authors upon reasonable demand.

### Ethics approval

This paper was published as partial fulfillment of the MSc student project "Investigating the effects of alginate hydrogels on differentiation capacity of spermatogonia stem cells through the autophagy Process" which was reviewed and approved on June 15, 2022, by the Research Ethics Committees of Laboratory Animals - Tabriz University of Medical Sciences (ethical code: IR.TBZMED.REC.1401.280).

### Funding

This study was supported by a grant (No: 69497) from Tabriz University of Medical Sciences.

### References

1. Bornstein M, Huber-Krum S, Norris AH, Gipson JD. Infertility and perceived chance of conception among men in Malawi. *Hum Fertil.* 2023; 26(3):504-511. doi: 10.1080/14647273.2023.2190042.
2. Tang N, Pei M, Liu H, Chen J, Wang Y, Xie L, et al. Infertility-related stress, and dyadic coping as predictors of quality of life: Gender differences among couples with infertility issues. *Int J Women's Health.* 2024; 26:16:1265-1276. doi: 10.2147/IJWH.S469513.
3. von Estorff F, Mochtar MH, Lehmann V, van Wely M. Driving factors in treatment decision-making of patients seeking medical assistance for infertility: a systematic review. *Hum Reprod Update.* 2024; 30(3):341-354. doi: 10.1093/humupd/dmae001.
4. Permata Arinda Putri AN, Nadhiroh SR. A Literature Review: Association between Obesity and Infertility in Productive-Aged Men. *Amerta Nutr.* 2024;8(2):318-327. doi: 10.20473/amnt.v8i2.2024.318 327.
5. Bhattacharya I, Sharma SS, Majumdar SS. Etiology of male infertility: an update. *Reprod Sci.* 2024; 31(4):942-965. doi: 10.1007/s43032-023-01401-x.
6. Simon L, Mariotti-Celis MS. Bioactive compounds as potential alternative treatments to prevent cancer therapy-induced male infertility. *Front Endocrinol (Lausanne).* 2024; 18:14:1293780. doi: 10.3389/fendo.2023.1293780.
7. Potiris A, Perros P, Drakaki E, Mavrogianni D, Machairiotis N, Sfakianakis A, et al. Investigating the association of assisted reproduction techniques and adverse perinatal outcomes. *J Clin Med.* 2024;13(2):328. doi: 10.3390/jcm13020328.
8. Saad EA, Hassan HA, Ghoneum MH, Alaa El-Dein M. Edible wild plants, chicory and purslane, alleviated diabetic testicular dysfunction, and insulin resistance via suppression 8OHdg and oxidative stress in rats. *PLoS One.* 2024;19(4):e0301454. doi: 10.1371/journal.pone.0301454.
9. Feng X, Matsumura T, Yamashita Y, Sato T, Hashimoto K, Odaka H, et al. In vitro spermatogenesis in isolated seminiferous tubules of immature mice. *PLoS One.* 2023;18(4):e0283773. doi: 10.1371/journal.pone.0283773.

10. Carrageta DF, Pereira SC, Ferreira R, Monteiro MP, Oliveira PF, Alves MG. Signatures of metabolic diseases on spermatogenesis and testicular metabolism. *Nat Rev Urol.* 2024;21(8):477-494. doi: 10.1038/s41585-024-00866-y.
11. Afzal A, Zhang Y, Afzal H, Saddozai UAK, Zhang L, Ji X-Y, et al. Functional role of autophagy in testicular and ovarian steroidogenesis. *Front Cell Dev Biol.* 2024; 12:1384047. doi: 10.3389/fcell.2024.1384047.
12. Esmailian Y, Hela F, Bildik G, İltumur E, Yusufoglu S, Yildiz CS, et al. Autophagy regulates sex steroid hormone synthesis through lysosomal degradation of lipid droplets in human ovary and testis. *Cell Death Dis.* 2023;14(5):342. doi: 10.1038/s41419-023-05864-3.
13. Rato L, Alves MG, Duarte AI, Santos MS, Moreira PI, Cavaco JE, et al. Testosterone deficiency induced by progressive stages of diabetes mellitus impairs glucose metabolism and favors glycogenesis in mature rat Sertoli cells. *Int J Biochem Cell Biol.* 2015;66:1-10. doi: 10.1016/j.biocel.2015.07.001.
14. Li J, You Y, Zhang P, Huang X, Dong L, Yang F, et al. Qiangjing tablets repair of blood-testis barrier dysfunction in rats via regulating oxidative stress and p38 MAPK pathway. *BMC Complement Med Ther.* 2022;22(1):133. doi: 10.1186/s12906-022-03615-z.
15. Yan H, Zhuang M, Xu X, Li S, Yang M, Li N, et al. Autophagy and its mediated mitochondrial quality control maintain pollen tube growth and male fertility in Arabidopsis. *Autophagy.* 2023;19(3):768-783. doi: 10.1080/15548627.2022.2095838.
16. Tian Y, Song W, Xu D, Chen X, Li X, Zhao Y. Autophagy induced by ROS aggravates testis oxidative damage in diabetes via breaking the feedforward loop linking p62 and Nrf2. *Oxid Med Cell Longev.* 2020;2020(1):7156579. doi: 10.1155/2020/7156579.
17. Salem M, Khadivi F, Javanbakht P, Mojaverrostami S, Abbasi M, Feizollahi N, et al. Advances of three-dimensional (3D) culture systems for in vitro spermatogenesis. *Stem Cell Res Ther.* 2023;14(1):262. doi: 10.1186/s13287-023-03466-6.
18. Izadpanah M, Del Bakhshayesh AR, Bahroudi Z, Seghinsara AM, Beheshti R, Mahdipour M, et al. Melatonin and endothelial cell-loaded alginate-fibrin hydrogel promoted angiogenesis in rat cryopreserved/thawed ovaries transplanted to the heterotopic sites. *J Biol Eng.* 2023;17(1):23. doi: 10.1186/s13036-023-00343-x.
19. Bashiri Z, Amiri I, Gholipourmalekabadi M, Falak R, Asgari H, Maki CB, et al. Artificial testis: a testicular tissue extracellular matrix as a potential bio-ink for 3D printing. *Biomater Sci.* 2021;9(9):3465-3484. doi: 10.1039/D0BM02209H.
20. Gieroba B, Przekora A, Kalisz G, Kazimierzczak P, Song CL, Wojcik M, et al. Collagen maturity and mineralization in mesenchymal stem cells cultured on the hydroxyapatite-based bone scaffold analyzed by ATR-FTIR spectroscopic imaging. *Mater Sci Eng C Mater Biol Appl.* 2021;119:111634. doi: 10.1016/j.msec.2020.111634.
21. Lin W, Zhang H, Zhang W, Qi H, Zhang G, Qian J, et al. In vivo degradation and endothelialization of an iron bioresorbable scaffold. *Bioact Mater.* 2021;6(4):1028-1039. doi: 10.1016/j.bioactmat.2020.09.020.
22. Morshedloo F, Khoshfetrat AB, Kazemi D, Ahmadian M. Gelatin improves peroxidase-mediated alginate hydrogel characteristics as a potential injectable hydrogel for soft tissue engineering applications. *J Biomed Mater Res B Appl Biomater.* 2020;108(7):2950-2960. doi: 10.1002/jbm.b.34625.
23. Yang Y, Lin Q, Zhou C, Li Q, Li Z, Cao Z, et al. A testis-derived hydrogel as an efficient feeder-free culture platform to promote mouse spermatogonial stem cell proliferation and differentiation. *Front Cell Dev Biol.* 2020;8:250. doi: 10.3389/fcell.2020.00250.

24. Vytla VS, Ochs RS. Metformin increases mitochondrial energy formation in L6 muscle cell cultures. *J Biol Chem.* 2013;288(28):20369-77. doi: 10.1074/jbc.M113.482646.
25. Cenac C, Ducatez M, F, Guéry JC. Hydroxychloroquine inhibits proteolytic processing of endogenous TLR7 protein in human primary plasmacytoid dendritic cells. *Eur J Immunol.* 2022;52(1):54-61. doi: 10.1002/eji.202149361.
26. Ma T, Tian X, Zhang B, Li M, Wang Y, Yang C, et al. Low-dose metformin targets the lysosomal AMPK pathway through PEN2. *Nature.* 2022;603(7899):159-165. doi: 10.1038/s41586-022-04431-8.
27. Nemati S, Alizadeh Sardroud H, Baradar Khoshfetrat A, Khaksar M, Ahmadi M, Amini H, et al. The effect of alginate–gelatin encapsulation on the maturation of human myelomonocytic cell line U937. *J Tissue Eng Regen Med.* 2019;13(1):25-35. doi: 10.1002/term.2765.
28. Sokouti Nasimi F, Zahri S, Ahmadian S, Bagherzadeh A, Nazdikbin Yamchi N, Haghighi L, et al. Estradiol modulated differentiation and dynamic growth of CD90+ spermatogonial stem cells toward Sertoli-like cells. *Life Sci.* 2021;286:120041. doi: 10.1016/j.lfs.2021.120041.
29. Rahbarghazi A, Siahkoughian M, Rahbarghazi R, Ahmadi M, Bolboli L, Mahdipour M, et al. Melatonin and prolonged physical activity attenuated the detrimental effects of diabetic condition on murine cardiac tissue. *Tissue Cell.* 2021;69:101486. doi: 10.1016/j.tice.2021.101486.
30. Abbasiliasi S, Shun TJ, Ibrahim TAT, Ismail N, Ariff AB, Mokhtar NK, et al. Use of sodium alginate in the preparation of gelatin-based hard capsule shells and their evaluation in vitro. *RSC Adv.* 2019;9(28):16147-16157. doi: 10.1039/c9ra01791g.
31. Pereira R, Tojeira A, Vaz DC, Mendes A, Bártolo P. Preparation and characterization of films based on alginate and aloe vera. *Int J Polym Anal Charact.* 2011;16(7):449-464. doi: 10.1080/1023666X.2011.599923.
32. Devi N, Hazarika D, Deka C, Kakati D. Study of complex coacervation of gelatin A and sodium alginate for microencapsulation of olive oil. *J Macromol Sci Part A.* 2012;49(11):936-945. doi: 10.1080/10601325.2012.722854.
33. Dong Z, Wang Q, Du Y. Alginate/gelatin blend films and their properties for drug controlled release. *J Membr Sci.* 2006;280(1-2):37-44. doi: 10.1016/j.memsci.2006.01.002.
34. Qin Y, Hu H, Luo A. The conversion of calcium alginate fibers into alginate acid fibers and sodium alginate fibers. *J Appl Polym Sci.* 2006;101(6):4216-4221. doi: 10.1002/app.24524.
35. Augst AD, Kong HJ, Mooney DJ. Alginate hydrogels as biomaterials. *Macromol Biosci.* 2006;6(8):623-633. doi: 10.1002/mabi.200600069.
36. Luginbuehl V, Wenk E, Koch A, Gander B, Merkle HP, Meinel L. Insulin-like Growth Factor I—Releasing Alginate-Tricalciumphosphate Composites for Bone Regeneration: Luginbuehl et al. *Pharm Res.* 2005;22(6):940-50. doi: 10.1007/s11095-005-4589-9.
37. Chen X, Wu T, Bu Y, Yan H, Lin Q. Fabrication and Biomedical Application of Alginate Composite Hydrogels in Bone Tissue Engineering: A Review. *Int J Mol Sci.* 2024; 25(14):7810. doi: 10.3390/ijms25147810.
38. Kavand A, Noverraz F, Gerber-Lemaire S. Recent advances in alginate-based hydrogels for cell transplantation applications. *Pharmaceutics.* 2024;16(4):469. doi: 10.3390/pharmaceutics16040469.
39. Chakraborty J, Ghosh S. Cellular proliferation, self-assembly, and modulation of signaling pathways in silk fibroin gelatin-based 3D bioprinted constructs. *ACS Appl Bio Mater* 2020;3(12):8309-8320. doi: 10.1021/acsabm.0c01252.
40. Kuai Z, Chao X, He Y, Ren W. Metformin attenuates inflammation and boosts autophagy in the liver and intestine of chronologically aged rats. *Exp Gerontol.* 2023;184:112331. doi: 10.1016/j.exger.2023.112331.

41. Liebl MP, Meister SC, Frey L, Hendrich K, Klemmer A, Wohlfart B, et al. Robust LC3B lipidation analysis by precisely adjusting autophagic flux. *Sci Rep.* 2022;12(1):79. doi: 10.1038/s41598-021-03875-8.
42. Tang J, Li Y, Xia S, Li J, Yang Q, Ding K, et al. Sequestosome 1/p62: A multitasker in the regulation of malignant tumor aggression (Review). *Int J Oncol.* 2021;59(4):77. doi: 10.3892/ijo.2021.5257.
43. Yim WW-Y, Mizushima NJCd. Lysosome biology in autophagy. *Cell Discov.* 2020;6(1):6. doi: 10.1038/s41421-020-0141-7.
44. Park H, Kim J, Shin C, Lee S. Intersection between Redox Homeostasis and Autophagy: Valuable Insights into Neurodegeneration. *Antioxidants (Basel).* 2021; 10(5):694. doi: 10.3390/antiox10050694.
45. Peng X, Zhang S, Jiao W, Zhong Z, Yang Y, Claret FX, et al. Hydroxychloroquine synergizes with the PI3K inhibitor BKM120 to exhibit antitumor efficacy independent of autophagy. *J Exp Clin Cancer Res.* 2021;40(1):374. doi: 10.1186/s13046-021-02176-2.
46. Adelipour M, Saleth LR, Ghavami S, Alagarsamy KN, Dhingra S, Allameh A. The role of autophagy in the metabolism and differentiation of stem cells. *Biochim Biophys Acta Mol Basis Dis.* 2022;1868(8):166412. doi: 10.1016/j.bbadis.2022.166412.
47. Hassanpour M, Rezabakhsh A, Pezeshkian M, Rahbarghazi R, Nouri M. Distinct role of autophagy on angiogenesis: highlights on the effect of autophagy in endothelial lineage and progenitor cells. *Stem Cell Res Ther.* 2018;9(1):305. doi: 10.1186/s13287-018-1060-5.
48. Kim J, Kundu M, Viollet B, Guan KL. AMPK and mTOR regulate autophagy through direct phosphorylation of Ulk1. *Nat Cell Biol.* 2011;13(2):132-41. doi: 10.1038/ncb2152.
49. Alruwaili M, Jarrar B, Jarrar Q, Alruwaili M, Goh KW, Moshawih S, et al. Hydroxychloroquine toxicity in the vital organs of the body: in vivo study. *Front Biosci (Landmark Ed).* 2023;28(7):137. doi: 10.31083/j.fbl2807137.
50. Li R-N, Zhu Z-D, Zheng Y, Lv Y-H, Tian X-E, Wu D, et al. Metformin improves boar sperm quality via 5'-AMP-activated protein kinase-mediated energy metabolism in vitro. *Zool Res.* 2020;41(5): 527-538. doi: 10.24272/j.issn.2095-8137.2020.074.
51. Zhang Y-L, Liu F, Li Z-B, He X-T, Li X, Wu R-X, et al. Metformin combats high glucose-induced damage to the osteogenic differentiation of human periodontal ligament stem cells via inhibition of the NPR3-mediated MAPK pathway. *Stem Cell Res Ther.* 2022;13(1):305. doi: 10.1186/s13287-022-02992-z.
52. Rotimi DE, Iyobhebhe M, Oluwayemi ET, Evbuomwan IO, Asaleye RM, Ojo OA, et al. Mitophagy and spermatogenesis: role and mechanisms. *Biochem and Biophys Rep.* 2024;38:101698. doi: 10.1016/j.bbrep.2024.101698.
53. Shang Y, Wang H, Jia P, Zhao H, Liu C, Liu W, et al. Autophagy regulates spermatid differentiation via degradation of PDLIM1. *Autophagy.* 2016;12(9):1575-92. doi: 10.1080/15548627.2016.1192750.
54. Naghibi M, Nasrabadi HT, Rad JS, Garjani A, Farashah MSG, Mohammadnejad D. Forskolin improves male reproductive complications caused by hyperglycemia in type 2 diabetic rats. *Int J Fertil Steril.* 2023;17(4): 268-275. doi: 10.22074/IJFS.2022.544368.1235.
55. Arab M, Naseri M, Shahi Sadr Abadi F, Nasri S. The Effect of Aerial Part of *Melissa Officinalis* L. Hydro-Alcoholic Extract on Pituitary- Gonadal Axis Function in Diabetic Male Mice. *J Nutr Food Secur.* 2024;9(4):599-608. doi: 10.18502/jnfs.v9i4.16888.
56. Tavares R, Escada-Rebelo S, Silva A, Sousa M, Ramalho-Santos J, Amaral S. Antidiabetic therapies and male reproductive function: where do we stand? *Reproduction.* 2018;155(1):R13-R37. doi: 10.1530/REP-17-0390.

57. Huang R, Chen J, Guo B, Jiang C, Sun W. Diabetes-induced male infertility: potential mechanisms and treatment options. *Mol Med.* 2024;30(1):11. doi: 10.1186/s10020-023-00771-x.
58. Bakhtyukov AA, Derkach KV, Sorokoumov VN, Steepochkina AM, Romanova IV, Morina IY, et al. The Effects of Separate and Combined Treatment of Male Rats with Type 2 Diabetes with Metformin and Orthosteric and Allosteric Agonists of Luteinizing Hormone Receptor on Steroidogenesis and Spermatogenesis. *Int J Mol Sci.* 2021; 23(1): 198. doi: 10.3390/ijms23010198.
59. Jin-yi F, GUO Z-x, Wen-jiao S, Ying-lun S, Li-li Y. Protective effect of recombinant spherical adiponectin on testis of diabetic mice by regulating autophagy and endoplasmic reticulum stress. *Jie Fang Jun Yi Xue Za Zhi.* 2019; (2019): 912-918. doi: 10.11855/j.issn.0577-7402.2019.11.03.
60. Mu Y, Yan W-j, Yin T-l, Zhang Y, Li J, Yang J. Diet-induced obesity impairs spermatogenesis: a potential role for autophagy. *Sci Rep.* 2017;7(1):43475. doi: 10.1038/srep43475.
61. Wang N, Zhou Y, Ngowi EE, Qiao A. Autophagy: Playing an important role in diabetes and its complications. *Med Drug Discov.* 2024;22(3):100188. doi: 10.1016/j.medidd.2024.100188.